The Neutrino Telescope ANTARES

Juan José Hernández-Rey (for the ANTARES collaboration)
IFIC – Instituto de Física Corpuscular, CSIC–Universitat de València,
apdo.22085, E46071–Valencia, Spain

May 25, 2004

Abstract.
Whilst the number of observed astrophysical sources of γ–rays is now moderately high, only three astrophysical objects have been studied with neutrinos, namely the Sun, a supernova (SN1987A) and the Earth (its atmosphere) However, astro–neutrinos may give a new boost to Astrophysics similar to the impressive progress provided during the last decades by γ–rays. The ANTARES collaboration aims to build a large neutrino telescope under the Mediterranean Sea at a depth of 2500 m. To reach this goal a remarkable effort of R&D has been performed in recent years that has culminated in the deployement, connection and operation of two prototype strings. The final detector will be composed of 12 strings and will be ready by 2006.

Keywords: Neutrino Telescope, High Energy Astrophysics

1. The link between γ and ν Astrophysics

There are only a few elementary particles at our disposal as cosmic messengers. The electromagnetic radiation has traditionally provided most of the astrophysical information and the advent of new detection techniques covering increasingly wider ranges of electromagnetic wavelengths has historically lead to the discovery of new phenomena or to a deeper understanding of already known astrophysical sources. A few decades ago γ–ray astrophysics “opened a new window to the Universe”, a most fruitful one for that matter. But in addition to photons, other messengers such as cosmic rays or neutrinos are available for the investigation of the Universe and deserve our attention.

The information obtained from the different cosmic messengers is to a certain extent complementary, in such a way that the limitations of one type of messenger or wavelength is overcome by another. This is particularly the case in the high energy regime, where cosmic-rays, γ–rays and neutrinos have features widely different. Protons and nuclei bring information of the most energetic astrophysical phenomena, but their trajectories are bent by magnetic fields, so that even in the presence of weak fields any directional information is lost, unless they come from short distances and have extremely high energies, according to the expression: $\theta(rad) \sim L(kpc) \cdot Z \cdot B(\mu G)/E(EeV)$, where θ, L, Z, B and E are the bending angle, the distance travelled, the electric charge, the magnetic field and the energy of the particle or nucleus in the units shown. Neutrons do not undergo deflection, but since they quickly decay they can hardly travel the distance that separates the Earth from the center of the Galaxy even with energies above a few EeV. Furthermore, at very high energies, cosmic–rays interact with the cosmic microwave background, so that the distance they can travel before being absorbed is limited and depends on their energy (the so–called GKZ limit). In the TeV region their mean free path is around a few tens of Mpcs (the Virgo cluster is at about 20 Mpcs) and at energies of the order of hundreds of TeV they can hardly reach the Earth travelling from the Galactic centre. Being electrically neutral, γ–rays do not suffer the deflection due to the magnetic fields. Nevetheless, at high energies they interact with the low energy photon soup present in the Universe (the infrared and cosmic microwave backgrounds), so that at a few TeV they travel in average a few tens of Mpcs, whilst in the $\sim$100 TeV region they can harldy fly 10 kpcs without being absorbed. Neutrinos, as γ–rays, are electrically neutral and stable. Moreover, due to their low probability of interaction they can come from very distant or very dense objects without being absorbed. A 50 TeV neutrino has an interaction length of the order of the Earth's diameter. Since neutrinos are part of the final debris of elementary particles in a number of processes, they are a very convenient tool to investigate high energy, long distance phenomena. The advantage of having a low interaction cross–section is at the same time a drawback from the experimental point of view: the detection of even the highest fluxes of neutrinos requires huge detectors.

Neutrino astrophysics does exist, but its realm reduces at present to the observation of three astrophysical objects: the Sun, a supernova (SN1987A) and the Earth (or more precisely, its atmosphere) and to the energy region spanning from a few MeV to a few tens of MeV. No matter how modest this may seem, the discoveries surrounding this neutrino observations have had a very important impact.

Several projects have been launched to detect cosmic neutrinos in wider energy ranges. To the first generation of high energy ($E>10$ GeV) neutrino telescopes, such as AMANDA and BAIKAL and the second wave of projects, such as ANTARES, NEMO or NESTOR, new initiatives to build yet bigger detectors such as IceCube or KM3 exist. Morevover, new ideas based on the detection of neutrinos through radiowaves or sound have been proposed and progress is being made in that front too.

Candidates for neutrino sources are in general also γ–ray sources, since most of the mechanisms that produce neutrinos also produce high energy photons and cosmic rays. Indeed, rather stringent limits on the diffuse neutrino flux are based on this connection (see section 5). Morevover, the possibility that the more energetic γ–rays are not produced through inverse Compton scattering, but in the decay of neutral pions produced in hadronic collisions could be clarified by the detection of neutrinos. Candidates for such processes are at present scarce and contested (Enomoto, 2002)(Reimer, 2002). It is natural to think that the understanding of astronomical objects such as active galactic nuclei or gamma ray bursts outside the Galaxy and supernova remnants, micro–quasars or pulsars in the Galaxy will greatly improve if an unambigous neutrino signal, no matter how faint, is detected.

2. The ANTARES neutrino telescope

The European collaboration ANTARES is currently building a neutrino detector under the Mediterranean Sea (Aslanides, 1999). Muonic neutrinos will be detected through the muons they produce when interacting with the matter that surrounds the detector. Even though this type of neutrinos are the main detection goal, electronic neutrinos will be detected too by the secondary electromagnetic showers they produce. Muons –and charged particles in general– will be detected through the Cherenkov light they emit when traversing the sea water. To this end, an array of photomultipliers (PMTs) will be distributed in a large volume of water. The ANTARES detector (see Figure 1) will consist of 12 strings (indistinctly called lines), with 25 storeys each. Each storey contains a triplet of 3 optical modules (OMs). An OM (Amram, 2002) consists in a pressure–resistant glass sphere housing a 10" PMT, its base and a LED for calibration purposes. The 3 OMs of a storey are angularly separated by 120 degrees in the horizontal plane and the axis of their PMTs are looking 45 degrees below the horizontal. A storey also holds a titanium container housing the front-end readout electronics of the PMT, an ethernet board for data acquisition, electronic boards for triggering and for clock distribution and a tiltmeter–compass to measure the angles of the storey. Some storeys also include a hydrophone for acoustic positioning and a LED optical beacon for timing calibration (Hernández-Rey, 2003a).

The distance between storeys of a string is 14.5 m, the first storey being located 100 m above the sea bed, so that the total height of each string is more than 450 m. The strings are anchored to the sea bed and held taut by means of a buoy at their top. At the bottom of each string there is a container housing the general electronics of the string, acoustic emitters for positioning and in some strings laser beacons for timing calibration. In addition to the 12 standard strings, the detector

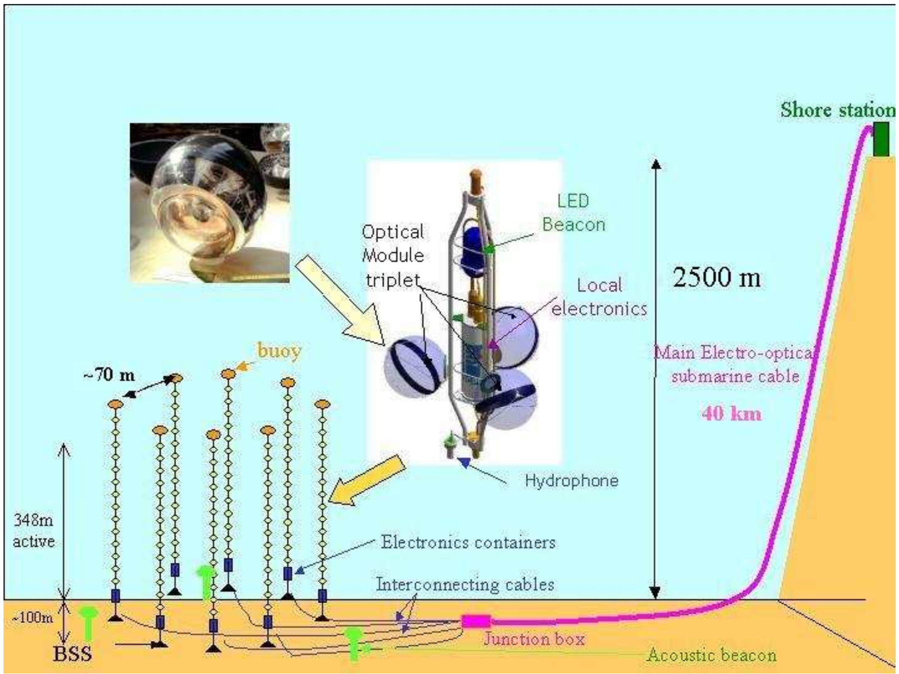

Figure 1. Scheme of the ANTARES detector. Inserted is a sketch of one of the 25 storeys that each string will hold. The total number of strings is 12 plus a special instrumentation line.

will also include a special intrumentation line that will support devices to monitor the main environmental parameters, such as the speed of the water currents, the sound velocity and optical properties of water, as the absorption length and will also act as a dedicated host for studies in other fields, such as marine Biology, Seismology and Oceanography. The strings lay on the sea floor separated from each other by $\sim$ 65 m in average and filling an octagonal surface.

The detector is located at a depth of 2500 m in the Mediterranean Sea (42°48'N,6°10'E), in front of Toulon in the south of France. This location provides a 3.5 π sr coverage of the sky and allows in particular the survey of the Galactic centre during 67% of the time.

The detector is controlled from the shore station situated at La-Seyne-sur-Mer, a village close to Toulon. A standard telecommunication electro–optical cable, 40 km in length, links the detector to the shore. This cable, that contains 48 optical fibres, provides a two–way communication tool to issue commands to and retrieve data from the detector and delivers the necessary electric power for its proper operation. The cable is linked in the sea bed of the ANTARES site to the junction box, the distributing device to which the strings are connected by several cables a few hundred meter long.

The shore station is currently operative, the electro-optical cable has been deployed and was connected to the junction box and is working steadily since almost one year and a half. Furthermore, two prototype strings were deployed, operated and recovered (see next section). The full detector is expected to be ready by 2006.

3. Progress and status of the project

The ANTARES collaboration had a first phase of R&D in which several studies were performed and prototypes built and deployed. During this phase, several versions of different autonomous strings were used in about fifty deployments. These strings, which sent the data to the surface by means of sonar devices or recorded them until their recovery, were used to measure in different sites several quantities, such as the optical properties of the surrounding water (Aguilar, 2004), the bio-fouling on optical surfaces and their subsequent loss of transparency (Amram, 2003) and the optical backgrounds due the decay of the radioactive salts present in sea water and to bio–luminescence (Amram, 2000). These studies lead to the selection of the present site, which was further investigated in terms of the geological characteristics of its ground (Amram, 2003) and inspected by means of a submarine in order to know in detail its orography and to spot all the objects present in the area.

From November 1999 to June 2000 a “demonstrator line” was deployed and operated in order to prove the feasibility of the project and to test several of its systems. The capability to deploy properly a long structure in the intended placed was proven with this line. The designed acoustic positioning system was shown to locate the OMs with a precision of 5 cm with respect to several points in the sea floor. Several thousand atmospheric muons were recorded and reconstructed.

The final electro-optical cable linking the shore and the ANTARES site was deployed in October 2001. Meanwhile, a small version of a detector string was built. This so–called Pre–production Sector Line (PSL) was composed of the anchor, five storeys and the buoy. It represents one fifth (“a sector”) of a full final line and constitutes its minimal functional unit concerning power distribution and data transmission. The line had 15 OMs in total, but it also contained all the types of components of a full line, such as the hydrophones of the acoustic positioning system, the tiltmeters/compasses and a LED optical beacon.

The PSL was finally assembled and tested in the laboratory during the Summer and Autumn of 2002.

A second line, called Mini–Instrumentation Line (MIL) was assembled and tested in November 2002. This line had two storeys, 100 m apart, which contained devices to measure environmental parameters, namely, a current profiler, a sound velocimeter, a conductivity and temperature probe and a light transmissiometer. The MIL also contained devices for acoustic positioning and inter–string timing calibration (a laser beacon and an LED optical beacon).

Starting from December 2003 and ending in March 2003 a series of major marine operations ended in the full installation of these two lines. This included the deployment of the Junction Box and its connection to the previously deployed electro–optical cable and the deployment of the PSL and MIL and their connection to the Junction Box by the manned submarine *Nautile*. Both lines were then recovered in May and July 2003. All these marine operations have factually proven the mastering of the deployment techniques.

With this set–up, around 130 Gb of data were recorded at the shore station in about 100 days of running, so that the front-end acquisition, the digital transfer, the slow control and the power distribution, among other systems, were thoroughly checked. Counting rates, line shape and several other control parameters (temperatures, power consumption, etc) were recorded and monitored. Two main problems appeared during operation: the failure of an optical fibre inside the cables of the lines, which prevented the transmission of the clock signal, and a water leak in an electronic container of the MIL. The first problem was due to the pressure–induced collapse of the plastic tube protecting the optical fibres and will be avoided in the future enclosing them in steel tubes. The second problem was due to a bad manufacturer's specification in the tolerance of the hole's dimension of a specific type of connector. This will be avoided in the future using other type of connectors with larger security margins.

The absence of a clock signal prevented us from having the timing of the OM signals synchronized at the nanosecond level, as it is needed to reconstruct muon tracks. Nevertheless, counting rates of the OMs were recorded during the whole data–taking period. The left plot in Figure 2 shows the median values of the rates in kHz recorded during periods of 15 minutes as a function of the date of data–taking for the three OMs of one of the storeys of the PSL. The right plot in Figure 2 shows the burst fraction of the same OMs as a function of data–taking date. The burst fraction is defined as the fraction of time (during the same 15 minute periods) that the rate is 20% higher than the median rate. In our previous measurements with stand-alone strings (Amram, 2000) the results showed that in addition to a continous baseline of 60 kHz due to ^{40}K decays slowly modulated possibly by bio–luminescence coming from bacteria, there were sudden bursts of several hundreds kHz lasting from seconds to minutes (possibly by bio–luminescence coming from larger animals). These new data confirm these measurements, but show a larger variability. Correlations between the burst fraction and the baseline rate or the water currents are also observed. This optical background is 50–70% of the time below 100 kHz, a rate acceptable for data–taking.

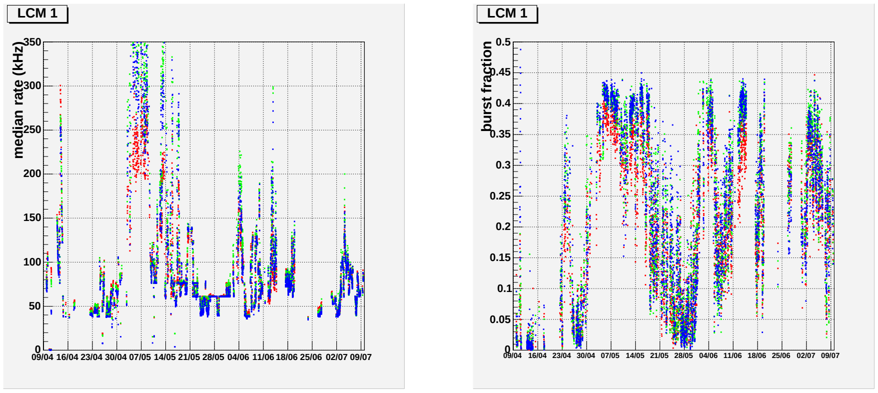

Figure 2. Median rate in kHz (left) and burst fraction in percentage (right) as a function of the data-taking date. See text for explanations.

4. Expected performances

The expected performances of the full 12–string detector have been estimated by computer simulation (Hernández-Rey, 2003b). The capabilities of the telescope can be characterized by several magnitudes. The muon effective area gives the ratio of the number of well reconstructed ("selected") muon events to the incoming muon flux. In Figure 3 the effective area for muons as a function of the parent neutrino energy is shown for an isotropic neutrino signal. Selection criteria have been applied in order to keep only well reconstructed tracks and to reject the atmospheric muon background (for other specific analyses, such as the search of point–like transient sources at known positions in the sky the criteria to be applied can be less stringent than those applied here). The upper curve (asterisks) represents all the events after reconstruction and selection. As can be seen, the effective area increases with energy and is somewhat lower than 0.1 km^2 for the highest energies. An indication of the angular resolution of the selected events is given by the lower curves in the same plot (triangles and stars), which correspond to those selected events that have an angle between the simulated and the reconstructed muon track smaller than 1° and 0.3°, respectively.

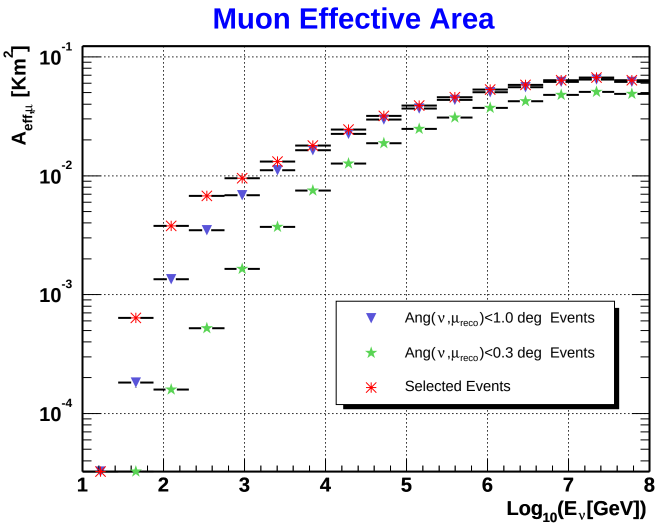

Figure 3. Effective area for muons as a function of the parent neutrino energy. Asterisks (upper curve) show the effective area for all the well-reconstructed ("selected") events, while triangles and stars (lower curves) show the effective area for those selected events for which the difference between the true and the reconstructed muon angle is smaller than 1° and 0.3°, respectively.

The angular resolution of the telescope is better seen in Figure 4, where the median of the distribution of the angular difference in space between the reconstructed muon track and *a*) the original parent neutrino (triangles) or *b*) the true muon track (squares) is shown as a function of the neutrino energy. The angle between the parent neutrino and the offspring muon dominates up to around 10 TeV. Above that energy, the instrumental resolution –which depends in particular on the effect of the scattering of light in water and on the overall timing resolution of the detector– is the limiting factor. A resolution of 0.15° can be reached. Note that a good angular resolution helps to reject the background in the case of point–like sources and is therefore of utmost importance in those studies where the source position is relevant. Due to the dependence of the resolution on the neutrino energy, the final resolution for a given source depends on its energy spectrum. The

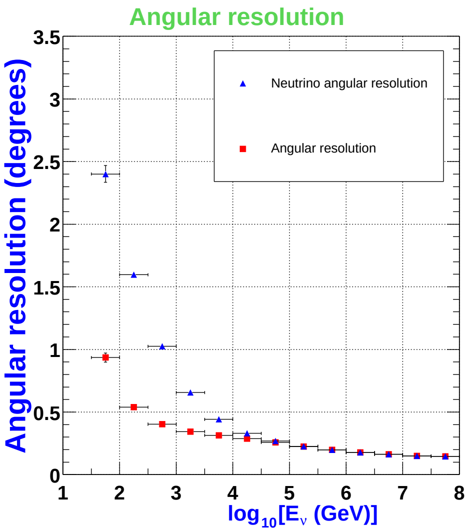

Figure 4. Angular resolution as a function of neutrino energy. The resolution is defined as the median of the distribution of the angle in space between the reconstructed muon and (a) the parent neutrino (triangles) or (b) the produced muon (squares).

hardest the spectrum, the better the resolution. For an E^{-2} spectrum, the neutrino angular resolution is 0.3 degrees.

The energy of the crossing muon can be estimated from the amount of light deposited in the PMTs. To this goal several estimators based on different techniques have been developed (Romeyer, 2003). Since the energy release from the muons at high energies has large fluctuations, a convenient magnitude is the logarithmic energy resolution, $log_{10}(\frac{\sigma_E}{E})$. Monte Carlo studies show that this resolution is between 0.2 and 0.3 for muons with energy above 1 TeV.

For muon energies below ∼200 GeV, the energy of the muon can be measured from its range in the water. This can be used to make neutrino oscillation studies in the 10–100 GeV muon energy range.

5. Sensitivity and predictions

There is a general consensus within the astro–neutrino community that the minimum scale of a neutrino telescope to gather the appropiate event statistics in a reasonable amount of time is of the order of the kilometer cube. This is based on two facts. From the theoretical point of view, the link between the extra–galactic sources of cosmic rays, gamma rays and neutrinos leads to severe limits on the neutrino diffuse flux expressed in the Waxman–Bahcall upper limit (W&B), $E^2\Phi < 4.5 \times 10^{-8}$ GeV cm^{-2} s^{-1} sr^{-1} (Waxman and Bahcall, 1998)(Bahcall and Waxman, 2001). This limit can be challenged –in more or less contrived scenarios– assuming that some of the required hypoteses do not hold (Mannheim, Protheroe and Rachen, 2000)(Kalashev et al., 2002). It nevertheless marks a limit for a list of first class candidate sources. Note that if oscillations with the present measured parameters are taken into account, the proportion of neutrino species emitted by these sources changes from $\nu_e : \nu_\mu : \nu_\tau = 1 : 2 :< 10^5$ to $\nu_e : \nu_\mu : \nu_\tau = 1 : 1 : 1$, so that predictions for muonic neutrinos are approximately a factor two smaller than above. The second recent reason to aim at km^3 volumes is that the AMANDA–II experiment has already set an upper limit on diffuse fluxes of $E^2\ \Phi < 8.6 \times 10^{-7}$ GeV cm^{-2} s^{-1} sr^{-1} in the energy range 50 TeV< E <5 PeV, assuming $\nu_e : \nu_\mu : \nu_\tau = 1 : 1 : 1$ and an E^{-2} spectrum (Ribordy, 2004).

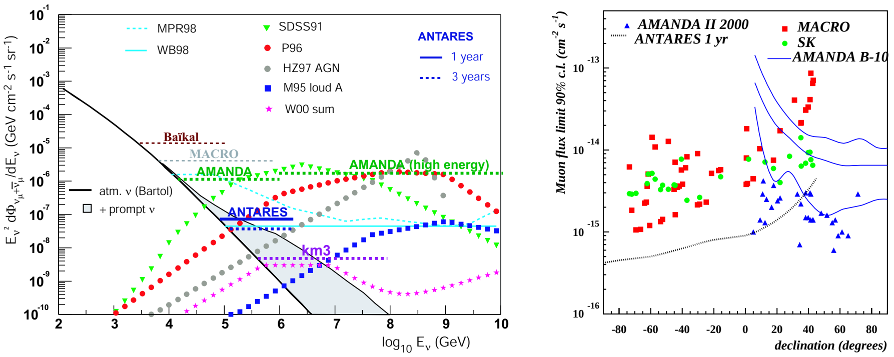

Figure 5. Left plot: Diffuse flux scaled to an E^{-2} spectrum as a function of the energy of the neutrino. The upper limits that can be set by ANTARES after one year (solid line) and three years (dashed line) of data–taking are indicated together with the expected atmospheric flux and some theoretical predictions are shown. Right plot: Sensitivity to point–like sources as a function of declination for different experiments expressed in terms of the 90% C.L. upper limit that they can set in case of a negative signal. See text for explanations and references.

For ANTARES, estimates by Monte Carlo simulation indicate that, after one year of data–taking and assuming an E^{-2} spectrum, the experiment will be able to set an upper limit for diffuse fluxes of $E^2\,\Phi < 7.8 \times 10^{-8}$ GeV cm^{-2} s^{-1} sr^{-1}, that will improve after three years of data–taking to $E^2\,\Phi < 3.9 \times 10^{-8}$ GeV cm^{-2} s^{-1} sr^{-1}, just below the W&B limit (see left plot in Figure 5). Nevertheless, this estimate does not take into account oscillations, which will worsen the limit by about a factor two if only muons are detected. However, in this case the detection of electromagnetic cascades can improve the limit by an amount not yet estimated. Although more detailed background studies are underway to confirm these numbers, they give an idea of the sensitivity of ANTARES to the diffuse flux, very close to beat the W&B limit.

The right plot in Figure 5 shows the 90% confidence level upper limit for muon fluxes (in $\mathrm{cm}^{-2}\ \mathrm{s}^{-1}$) from point–like sources as a function of the declination of the source for different experiments. The triangles are the upper limit set by the AMANDA II experiment for northern declinations (Ahrens, 2004). Previous results of AMANDA B–10 can be found in (Ahrens, 2003). The limits that ANTARES will set after one year of data–taking will clearly improve those of SuperKamiokande and MACRO in the southern hemisphere and are comparable to those of AMANDA II in the region of the sky where they overlap.

6. Conclusions and Outlook

The ANTARES collaboration has deployed and operated two prototype strings in the Mediterranean Sea at a depth of 2500 m. The production and installation phase of this neutrino telescope has started. The full 12–string detector is expected to be in place in 2006. By then, this telescope will be able to explore the Southern hemisphere in the search for extra–terrestrial neutrinos with a sensitivity much better than any other experiment before. In the meanwhile, new steps will be taken in a still larger scientific collaboration to design a km^3 detector in the Mediterranean Sea.

Acknowledgements

Financial support for the ANTARES project is provided by the following funding agencies: Commisariat à l'Energie Atomique, Centre Nationale de la Recherche Scientifique, European Commission (FEDER fund), Département du Var, Région P.A.C.A. et city of La Seyne–sur–Mer, France; Ministerio de Educación y Ciencia, Spain (FPA2003–00531); Istituto Nazionale de Fisica Nucleare, Italy; the Russian Foundation for Basic Research, Russia; the Foundation for Fundamental Research on Matter FOM and the National Scientific Research Organization NWO, The Netherlands.

References

Aguilar, J. A. *et al.* (2004) , Transmission of light in deep sea water at the site of the ANTARES neutrino telescope. submitted to *Astropart. Phys.*

Ahrens, J. *et al.* (2003), Search for point sources of high–energy neutrinos with AMANDA. *Astrophys. J.*, 583:1040–1057, 2003.

Ahrens, J. *et al.* (2004) , Search for extraterrestrial point sources of neutrinos with AMANDA–II. *Phys. Rev. Lett.*, 92:071102-1–5, 2004.

Amram, P. *et al.* (2000) , Background light in potential sites for the ANTARES undersea neutrino telescope. *Astropart. Phys.*, 13:127–136, 2000.

Amram, P. *et al.* (2002) , The ANTARES optical module. *Nucl. Instrum. & Meth.*, A484:369–383, 2002.

Amram, P. *et al.* (2003) , Sedimentation and fouling of optical surfaces at the ANTARES site. *Astropart. Phys.*, 19:253–267, 2003.

Aslanides, E. et al. 1999), A deep sea telescope for high energy neutrinos. *astro-ph/9907432.*

Bahcall J. and Waxman, E. (2001), High energy astrophysical neutrinos: the upper bound is robust *Phys. Rev.* D64:023002-1–8, 2001.

Enomoto, R. *et al.* (2002), The Acceleration of Cosmic-ray Protons in the Supernova Remnant RX J1713.7-3946. *Nature* 416:823–826, 2002.

Hernández-Rey, J. J. (2003a), Timing calibration of the ANTARES neutrino telescope. Proceedings of the *28th International Conference on Cosmic Rays*, 3:1537–1540, 2003.

Hernández-Rey, J. J. (2003b), Expected performances of the future neutrino telescope ANTARES. *Nuclear Physics B (Proc. Suppl.)*, 114:211–216, 2003.

Kalashev O.E. *et al.*, Ultrahigh–energy neutrinos and their constraints. *Phys. Rev.* D66:063004-1–11, 2002.

Mannheim K., Protheroe R.J. and Rachen J.P. (2000), Cosmic ray bounds for models of extragalactic neutrino production. *Phys. Rev.* D63:023003-1–16, 2000.

Reimer O. and Pohl, M. (2002), No evidence yet for hadronic TeV gamma–ray emission from RX J1713.7-3946. *Astronom. & Astrophys.* 390:L43–L46, 2002.

Romeyer A., Bruijn R. and Zornoza J. de D. (2003), Muon energy reconstruction in ANTARES and its application to the diffuse neutrino flux. Proceedings of the *28th International Conference on Cosmic Rays*, 3:1329–1332, 2003.

Ribordy, M. (2004), AMANDA: status and latest results. *hep–ex/0405035* and references therein.

Waxman, E. and Bahcall J. (1998), High energy neutrinos from astrophysical sources: an upper bound. *Phys. Rev.* D59:023002-1–8, 1998.